THE JOURNAL OF PHYSICAL CHEMISTRY A

Article

pubs.acs.org/JPCA

Structures and Electronic Properties of $(KI)_n^{-/0}$ (n = 1−4) and $K(KI)_n^{-/0}$ (n = 1−3) Clusters: Photoelectron Spectroscopy, Isomer-Depletion, and ab Initio Calculations

Gao-Lei Hou, Gang Feng, Li-Juan Zhao, Hong-Guang Xu, and Wei-Jun Zheng*

Beijing National Laboratory for Molecular Sciences, State Key Laboratory of Molecular Reaction Dynamics, Institute of Chemistry, Chinese Academy of Sciences, Beijing 100190, China

Supporting Information

ABSTRACT: The $(KI)_n^-$ (n = 1−4) and $K(KI)_n^-$ (n = 1−3) clusters were studied by negative ion photoelectron spectroscopy and ab initio calculations. Comparison between the theoretical vertical detachment energies and the experimental values revealed that multiple isomers may coexist in the experiments. The existence of two isomers for $K(KI)^-$ and $K(KI)_2^-$ were confirmed directly by isomer-depletion experiments, in which the low adiabatic detachment energy isomers were depleted by a 1064 nm laser beam before the anions were photodetached by a 532 nm laser beam. Our results show that the most stable structures of the $K(KI)^-$, $(KI)_2^-$, and $K(KI)_2^-$ anions are chain structures, while those of their neutral counterparts are planar. Three-dimensional structures start to appear at n = 3 for $(KI)_n^{-/0}$ and $K(KI)_n^{-/0}$. In the $K(KI)_n^-$ cluster anions, the excess electron is localized on the extra K atom and forms an electron pair with the existing s electron of the K atom; the resulting negatively charged K prefers to interact with the other positively charged K atoms rather than with the I atoms. Both the anionic and neutral $(KI)_4$ clusters have cuboid structures, which may be regarded as the smallest structural motif of KI crystal.

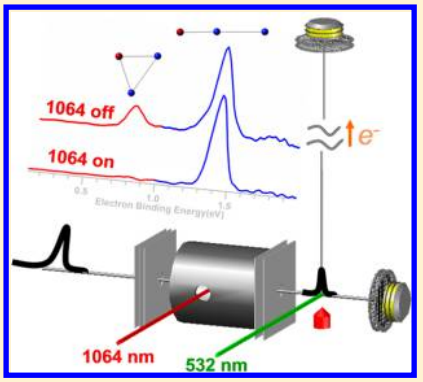

1. INTRODUCTION

Alkali-halide clusters have been studied extensively in the past decades because of their simplicity and importance for understanding the transition of ionic-compound properties from microscale to macroscale.[1−8] The experiments[2,3] and theoretical calculations[4−8] suggested that the most stable structures of the large salt clusters with the stoichiometric $(MX)_n$ or nonstoichiometric $(MX)_nM^+$ and $(MX)_nX^-$ (M = alkali metal, X = halogen) form favor cuboid morphology. Investigation of salt clusters provides the opportunity to explore the growth mechanism of salt crystals and the evolution of salt bulk properties. Owing to the importance of salt clusters, they were investigated by a number of experimental techniques in recent years. For example, Veličković and co-workers studied the ionization energies of K_2X (X = F, Cl, Br, I),[9] K_nCl (n = 2−6), and K_nCl_{n-1} (n = 3 and 4)[10] clusters by thermal ionization mass spectrometry and found that all these clusters have lower ionization energies than K atom does (4.34 eV). Ohshimo et al. found non-rock-salt structures in sodium fluoride cluster ions using ion mobility mass spectrometry.[11] Daxner et al. investigated the self-assembly of NaF nanocrystals from chemical reactions between Na atoms and SF_6 molecules inside helium droplets using electron impacting and mass spectrometry.[12] Mass-selected anion photoelectron spectroscopy has long been used to study the structural evolution of salt clusters. Yang et al. utilized photoelectron spectroscopic technique to investigate the structural evolution of the stoichiometric sodium chloride cluster anions $(NaCl)_n^-$ (n = 2−22) produced by laser vaporization.[13] Wang and co-workers studied MX_2^- (M = Li, Na; X = Cl, Br, I)[14] and $Na_xCl_{x+1}^-$ (x = 1−4)[15] clusters by negative ion photoelectron spectroscopy and theoretical calculations. Smalley and co-workers[16] conducted photoelectron spectroscopy and photofragmentation studies on $(KI)_n^-$, $K(KI)_n^-$, and $K_2(KI)_n^-$ (n up to 13) clusters and suggested that the excess electrons in these clusters are all loosely bound and electron spin pairs may be formed in the K-rich clusters. Bloomfield and co-workers[17] conducted photoelectron spectroscopy experiment on the nonstoichiometric metal-rich alkali-halide clusters, $(NaCl)_3Na_m^-$ and $(KI)_3K_m^-$ (m = 0−5). They found some evidence of metal−nonmetal transition in these clusters with variation of cluster sizes or compositions.

Although the $(KI)_n^-$ and $K(KI)_n^-$ clusters have been investigated by Smalley, Bloomfield, and their co-workers previously, the detailed structures of $(KI)_n^{-/0}$ and $K(KI)_n^{-/0}$ have not been reported, and the possible existence of multiple isomers has not been investigated by experiment or theory in the literature. To better understand the structures and electronic properties of small potassium-iodide clusters, in this work, we investigated $(KI)_n^-$ (n = 1−4) and $K(KI)_n^-$ (n = 1−3) clusters using photoelectron spectroscopy. We confirmed the existence of multiple isomers for $K(KI)_n^-$ (n = 1−2) and

Received: September 21, 2015
Revised: October 16, 2015
Published: October 16, 2015

DOI: 10.1021/acs.jpca.5b09205
J. Phys. Chem. A 2015, 119, 11154−11161

$(KI)_n^-$ (n = 3−4) directly by isomer-depletion experiments or by changing source conditions. The structures of $(KI)_n^-$, $K(KI)_n^-$, and their neutral counterparts were investigated in detail with ab initio calculations, and the photoelectron peaks were assigned based on the comparison between experiment and theory. The results indicate that the excess electron has a large influence on the structures of salt clusters. The results also show that the existence of different isomers cannot be ignored even for small clusters composed of only three atoms.

2. EXPERIMENTAL AND THEORETICAL METHODS

2.1. Experimental Methods. The experiments were conducted on a home-built apparatus consisting of a time-of-flight (TOF) mass spectrometer and a magnetic-bottle photoelectron spectrometer, which has been described previously.[18] Briefly, the potassium-iodide clusters were produced in a laser vaporization source, in which a rotating and translating KI disk target was ablated by the second harmonic (532 nm) light pulses from a Nd:YAG laser, while helium carrier gas with ∼4 atm backing pressure was allowed to expand through a pulsed valve to cool the clusters. The cluster anions were mass analyzed by the TOF mass spectrometer. The $(KI)_n^-$ (n = 1−4) and $K(KI)_n^-$ (n = 1−3) clusters were each mass-selected and decelerated before being photodetached by the 266, 532, and/or 1064 nm photons from another Nd:YAG laser. The photodetached electrons were energy-analyzed by the magnetic-bottle photoelectron spectrometer. The photoelectron spectra were calibrated with the spectra of K^-, Cs^-, and Bi^- taken at similar conditions. The instrumental resolution was approximately 40 meV for electrons with 1 eV kinetic energy.

In order to provide direct experimental evidence for the coexistence of different isomers for $K(KI)^-$ and $K(KI)_2^-$, we conducted a isomer-depletion experiment which is similar to the "hole-burning" experiment reported by Akin and Jarrold.[19] A schematic diagram of the isomer-depletion experiment is shown in Figure 1. In the experiment, the mass-selected cluster anions were crossed with an isomer-depletion laser beam at the isoelectric region of the momentum decelerator. The isomer-depletion laser beam, which is 1064 nm in this work, is able to photodetach the low adiabatic detachment energy (ADE) isomers but cannot photodetach the high-ADE isomers. After depletion, the remaining cluster anions were decelerated by the momentum decelerator, reached the photodetachment region of the photoelectron spectrometer, and were crossed with a laser beam of shorter wavelength (higher photon energy), which is 532 nm in this work. The resulting electrons from the shorter wavelength were energy-analyzed by the photoelectron spectrometer. By this way, the photoelectron spectral features of the low-ADE isomers were depleted significantly in the collected spectra.

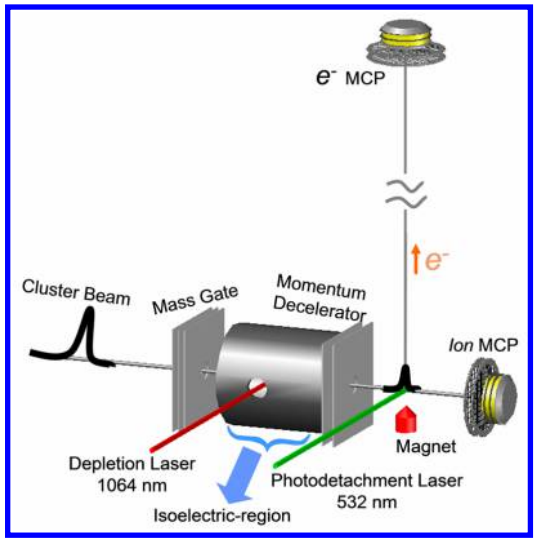

Figure 1. Schematic diagram of the isomer-depletion experiment.

2.2. Theoretical Methods. The theoretical calculations were performed with GAUSSIAN09 program package.[20] The structures of $(KI)_n^-$ (n = 1−4) and $K(KI)_n^-$ (n = 1−3) clusters as well as their neutrals were fully optimized with density functional theory (DFT) employing the B3LYP exchange-correlation functional.[21,22] The Pople's all-electron basis set 6-311+G(d) was used for K atom,[23,24] and the effective core potential (ECP) basis set LANL2DZ obtained from the EMSL basis set exchange was used for I atom.[25] Various initial structures have been considered in order to obtain the global minimum structure of each size cluster. Harmonic vibrational frequencies were calculated to make sure that the optimized structures are the real minima. The theoretical vertical detachment energies (VDEs) were calculated as the energy differences between the neutrals and the anions both at the anionic geometries. The theoretical ADEs were calculated as the energy differences between the neutrals and the anions with the neutrals relaxed to the nearest local minima using the geometries of the anions as initial structures. In order to obtain more accurate relative energies and VDEs, single-point energy calculations were performed using the CCSD(T) method with the same basis sets as those for the B3LYP functional. The relative energies and theoretical ADEs have been corrected by zero-point vibrational energies obtained with B3LYP functional. The following discussions are based on the relative energies and VDEs obtained with the CCSD(T) method unless otherwise specified.

3. EXPEIMENTAL RESULTS

Figure 2 presents the photoelectron spectra of $(KI)_n^-$ (n = 1−4) and $K(KI)_n^-$ (n = 1−3) clusters recorded with 532 nm photons. For KI^-, $(KI)_3^-$, and $(KI)_4^-$, the 1064 nm spectra were also recorded and presented in Figure 3. The 266 nm spectra of these clusters are shown in Figure S1 of the Supporting Information. No vibrational structure is resolved in the spectra of these clusters except the 1064 nm spectrum of KI^-. Thus, the ADE of each cluster is determined by drawing a straight line along the leading edge of the spectral features and adding the instrumental resolution to the crossing point with the binding energy axis to account for the spectral broadening. The VDEs are obtained from the maxima of the spectral features. The experimental VDEs and ADEs are summarized in Table 1.

Except $K(KI)^-$, all the other clusters investigated in this work have been previously studied by Smalley and co-workers using photoelectron spectroscopy.[16] Overall, our spectra are in agreement with theirs but with improved resolution. The 532 nm spectrum of KI^- has a broad feature at about 0.77 eV, which can be discernibly resolved into several fine structures with even spacing of 183 ± 40 cm^{-1} in its 1064 nm spectrum. This frequency corresponds to the K−I stretching vibration of neutral KI and is in good agreement with the value of 173 cm^{-1} measured by Rice and Klemperer.[26] The ADE of KI^- or the

DOI: 10.1021/acs.jpca.5b09205
J. Phys. Chem. A 2015, 119, 11154−11161

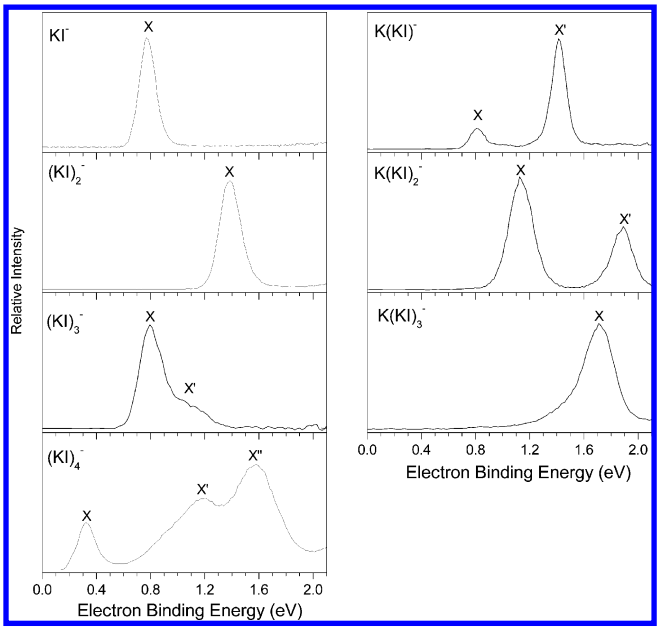

Figure 2. Photoelectron spectra of $(KI)_n^-$ (n = 1−4) and $K(KI)_n^-$ (n = 1−3) clusters at 532 nm.

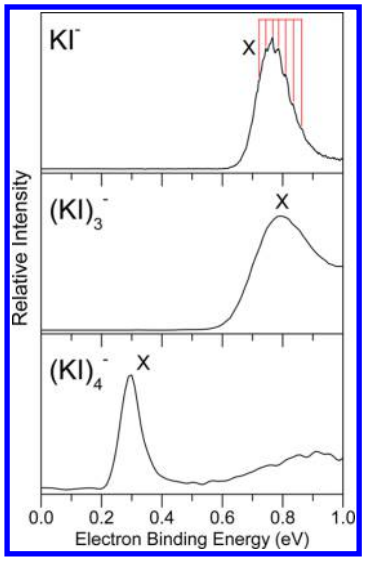

Figure 3. Photoelectron spectra of KI^-, $(KI)_3^-$, and $(KI)_4^-$ clusters at 1064 nm.

electron affinity (EA) of KI is determined from the 0−0 transition to be 0.72 ± 0.03 eV, in good agreement with the value of 0.728 ± 0.010 eV measured by Lineberger and co-workers.[27]

The 532 nm spectrum of $K(KI)^-$ shows one main feature (X′) at about 1.41 eV and a small feature (X) at about 0.78 eV. In the 532 nm spectrum of $(KI)_2^-$, there is only one feature centered at about 1.38 eV. The 532 nm spectrum of $K(KI)_2^-$ has two features at 1.13 (X) and 1.89 (X′) eV, respectively. For $(KI)_3^-$, there is a main feature at about 0.79 eV (X) and a weak feature at about 1.08 eV (X′). The relative intensities between the X and X′ features varied at different experimental conditions with the X′ features being lower at better source-cooling condition (Figure S2), indicating the X and X′ features might come from different isomers whose relative populations in the cluster beam changed at different experimental conditions. The spectrum of $K(KI)_3^-$ has a long rising onset and a main feature at around 1.71 eV. The 532 nm spectrum of $(KI)_4^-$ has a peak centered at 0.30 eV and two other features with maxima at about 1.19 and 1.58 eV, respectively. Similar to the case of $(KI)_3^-$, the relative intensities of these three features changed at different experimental conditions (Figure S3), indicating that these features might come from different isomers. As it will be shown later, the neutral $(KI)_3$ and $(KI)_4$ clusters both have closed shell electronic structures and thus should have large HOMO−LUMO gaps. Hence, the higher EBE spectral features of $(KI)_3^-$ and $(KI)_4^-$ in Figure 2 cannot correspond to the excited states of their neutrals. This also implies that they come from the different isomers in the cluster beams.

4. THEORETICAL RESULTS AND DICUSSIONS

Figures 4 and 5 present the most stable structures and typical low-lying isomers of $(KI)_n^-$ (n = 1−4) and $K(KI)_n^-$ (n = 1−3) clusters as well as their neutrals, respectively. More isomers are available in Figures S4 and S5 in the Supporting Information. Table 2 summarizes the theoretical VDEs and ADEs of these optimized isomers.

4.1. $(KI)_n^{-/0}$ (n = 1−4). The K−I bond length and stretching frequency of KI^- are calculated to be ∼3.28 Å and ∼130 cm^{-1}, respectively, in good agreement with the values of 3.250 Å and 140 cm^{-1} reported by Lineberger and co-workers.[27] The theoretical VDE of KI^- is calculated to be 0.66 eV, in agreement with the experimental result of 0.77 eV in Figure 2. For KI neutral, the K−I bond length is calculated to be 3.08 Å, in good accordance with the experimental value of 3.048 Å determined from microwave spectroscopy.[28] The K−I bond length of KI neutral is shorter than that of KI^- anion by 0.2 Å,

Table 1. Experimental VDEs and ADEs of $(KI)_n^-$ (n = 1−4) and $K(KI)_n^-$ (n = 1−3) Clusters from Their Photoelectron Spectra[a]

	X		X′		X″	
	ADE	VDE	ADE	VDE	ADE	VDE
KI^-	0.72(3)[b]	0.77(3)[b]				
$K(KI)^-$	0.73(5)	0.78(5)	1.34(5)	1.41(5)		
$(KI)_2^-$	1.28(5)	1.38(5)				
$K(KI)_2^-$	1.00(5)	1.13(5)	1.75(5)	1.89(5)		
$(KI)_3^-$	0.67(8)[b]	0.79(8)[b]	–	1.08(8)		
$K(KI)_3^-$	1.47(8)	1.71(8)				
$(KI)_4^-$	0.28(5)[b]	0.30(5)[b]	–	1.19(10)	–	1.58(8)

[a]All energies are in eV. The numbers in the parentheses represent the experimental uncertainty in the last digits. [b]For those clusters whose 1064 nm spectra are available, the experimental values are measured from the 1064 nm spectra.

DOI: 10.1021/acs.jpca.5b09205
J. Phys. Chem. A 2015, 119, 11154−11161

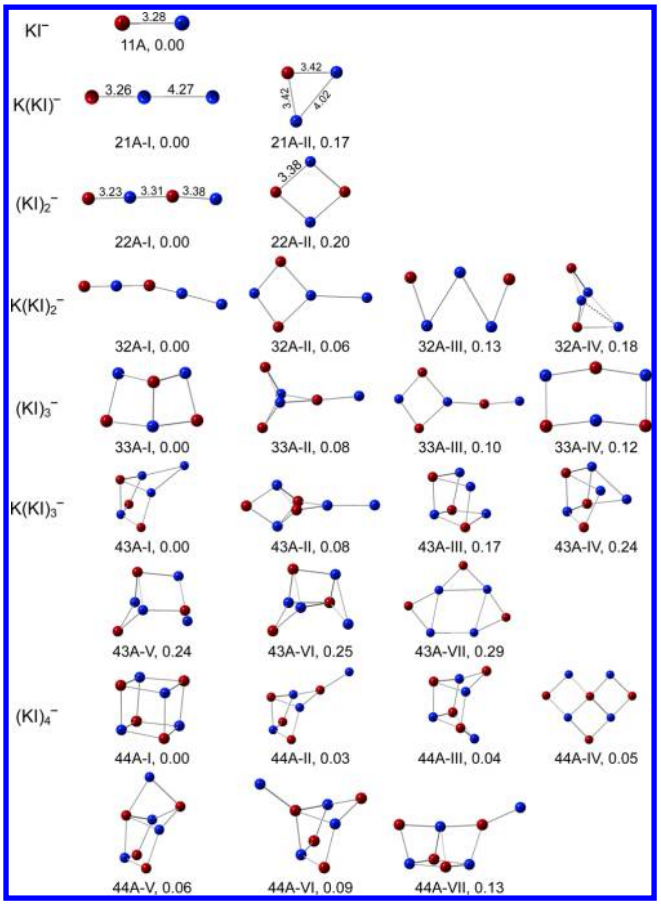

Figure 4. Most stable and typical low-lying energy isomers of $(KI)_n^-$ (n = 1−4) and $K(KI)_n^-$ (n = 1−3) clusters. Relative energies (in eV) are provided. The blue and purple balls represent K and I atoms, respectively.

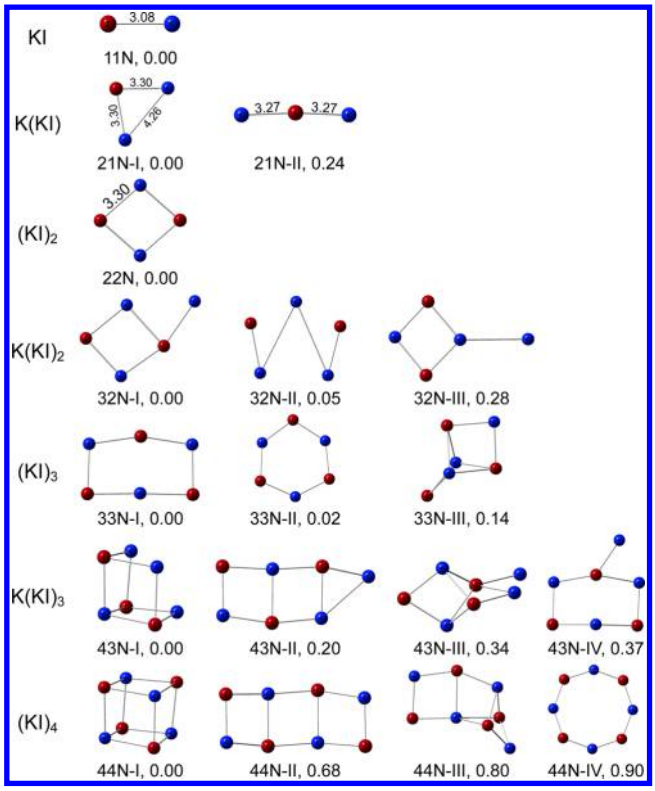

Figure 5. Most stable and typical low-lying energy isomers of $(KI)_n$ (n = 1−4) and $K(KI)_n$ (n = 1−3) neutrals. Relative energies (in eV) are provided. The blue and purple balls represent K and I atoms, respectively.

indicating that the interaction between K and I atoms is stronger in the neutral state than in the anionic state. This is consistent with the natural bond orbital (NBO) charge distributions as will be discussed below that the K atom in the KI^- anion is negatively charged (−0.107 e), whereas in the neutral KI it is positively charged (+0.854 e). The K−I stretching frequency of KI neutral is calculated to be ∼179 cm^{-1}, in agreement with the value of 173 cm^{-1} from IR measurement[26] as well as the current experimental result of 183 cm^{-1}. The good agreement between the calculated structures and energetics of $KI^{-/0}$ and the experiments shows the reliability of the current theoretical method.

The most stable structure of $(KI)_2^-$ is optimized to be quasi-linear (**22A-I**) and has a theoretical VDE of 1.24 eV, agreeing well with the experimental value of 1.38 eV. Isomer **22A-II** is a rhombus structure higher in energy than **22A-I** by 0.20 eV. Its theoretical VDE is calculated to be 0.13 eV, much lower than the experimental value. Thus, isomer **22A-I** is the most probable one detected in our experiments. The low VDE of isomer **22A-II** is similar to the previous theoretical calculations on the rhombus structure of $(NaCl)_2^-$, which found the rhombus structure of $(NaCl)_2^-$ has a low VDE of about 1270 cm^{-1} (∼0.16 eV).[29,30] Similarly, the VDE of the rhombus structure of $(KCl)_2^-$ is calculated to be 0.09 eV and has been attributed to a quadrupole-bound state by Gutsev et al.[31] The ground state structure of neutral $(KI)_2$ is a rhombus structure similar to **22A-II** but with slightly shorter K−I bond length (3.30 vs 3.38 Å). This structure is quite different from the ground state structure of its anionic counterpart **22A-I**, which is quasi-linear as described above. According to the previous studies on $(NaCl)_2^-$,[29,30] when the excess electron was added to the rhombus $(NaCl)_2$, the structure may rearrange into quasi-linear configuration by overcoming a small kinetic barrier of 0.108 eV (2.49 kcal/mol), due to the balance between the strength of the electron binding to the cluster and the coulomb repulsion between the neutral NaCl molecules. The case of $(KI)_2^{-/0}$ should be similar as that of $(NaCl)_2^{-/0}$.

In Figure 4, four low-lying isomers are shown for $(KI)_3^-$. The most stable one has an open-book-shaped structure. Its VDE is calculated to be 0.88 eV, in agreement with the experimental value of the X feature (0.79 eV). The other three isomers are 0.08, 0.10, and 0.12 eV higher in energy than the most stable one, and their VDEs are calculated to be 1.29, 1.06, and 0.31 eV, respectively. The VDEs of isomers **33A-II** and **33A-III** both agree with the VDE of the X′ feature (1.08 eV). Therefore, we suggest that isomers **33A-I**, **33A-II**, and **33A-III** may all exist in the experiments with **33A-I** contributing to the X feature and **33A-II** and **33A-III** contributing to the X′ feature, consistent with the variation of the relative intensities between the X and X′ features at different experimental conditions as discussed in Section 3. The first two stable isomers of neutral $(KI)_3$ shown in Figure 5 are nearly degenerate in energy with isomer **33N-II** being only 0.02 eV above isomer **33N-I**. Isomer **33N-I** is similar to **33A-I** with a tiled open book-shaped structure, and isomer **33N-II** is a hexagonal cyclic structure.

In Figure 4, seven low-lying isomers of $(KI)_4^-$ are presented. The most stable one (**44A-I**) is a cubic structure with a theoretical VDE of 0.05 eV. This ground state structure is

DOI: 10.1021/acs.jpca.5b09205
J. Phys. Chem. A 2015, 119, 11154−11161

Table 2. Theoretical VDEs and ADEs of the Most Stable and Typical Low-Lying Isomers of $(KI)_n^-$ (n = 1−4) and $K(KI)_n^-$ (n = 1−3) Clusters and Their Comparison with Experimental Results[a]

		ΔE		ADE		VDE		
				theo.	expt.	theo.		expt.
clusters		CCSD(T)	B3LYP	B3LYP		B3LYP	CCSD(T)	
KI^-	**11A**	0.00	0.00	0.84	0.72	0.89	0.66	0.77
$K(KI)^-$	**21A-I**	0.00	0.00	1.47	1.34	1.52	1.34	1.41
	21A-II	0.17	0.17	0.81	0.73	0.84	0.68	0.78
$(KI)_2^-$	**22A-I**	0.00	0.00	0.58	1.28	1.55	1.24	1.38
	22A-II	0.20	0.07	0.51		0.52	0.13	
$K(KI)_2^-$	**32A-I**	0.00	0.01	1.01	1.75	1.99	1.74	1.89
	32A-II	0.06	0.10	1.10	1.00	1.18	1.00	1.13
	32A-III	0.13	0.00	1.02		1.25	0.88	
	32A-VI	0.18	0.14	0.81		1.01	0.76	
$(KI)_3^-$	**33A-I**	0.00	0.00	0.73	0.67	1.20	0.88	0.79
	33A-II	0.08	0.16	0.68		1.60	1.29	1.08
	33A-III	0.10	0.16	0.57		1.36	1.06	
	33A-IV	0.12	0.02	0.70		0.75	0.31	
$K(KI)_3^-$	**43A-I**	0.00	0.00	1.34	1.47	1.85	1.63	1.71
	43A-II	0.08	0.12	1.43		1.53	1.33	
	43A-III	0.17	0.10	0.86		0.99	0.67	
	43A-IV	0.24	0.16	1.14		1.29	0.98	
	43A-V	0.24	0.16	0.80		1.29	0.98	
	43A-VI	0.25	0.22	1.09		1.31	1.05	
	43A-VII	0.29	0.20	1.22		1.72	1.39	
$(KI)_4^-$	**44A-I**	0.00	0.00	0.42	0.28	0.42	0.05	0.30
	44A-II	0.03	0.09	0.33	1.18	1.83	1.50	1.58
	44A-III	0.04	0.10	0.32		0.95	0.63	
	44A-IV	0.05	0.09	1.25		1.76	1.46	
	44A-V	0.06	0.11	1.17	0.67	1.41	1.09	1.19
	44A-VI	0.09	0.15	1.13		1.91	1.57	
	44A-VII	0.13	0.22	0.20		1.76	1.43	

[a]Relative energies of the isomers are also given. The structures labeled in bold represent the most probable ones observed in the experiments. All energies are in eV.

consistent with the previous suggestion.[16] However, the deviation between its theoretical VDE with the experimental value (0.30 eV) is relatively larger than those of the other size clusters, which probably can be attributed to the inability of the Lanl2DZ basis set used for I to describe the highly delocalized nature of the excess electron in the cubic $(KI)_4^-$. Isomer **44A-II** can be derived from **33A-I** by attaching KI to **33A-I** with its I atom interacting with the two less coordinated (to I atom) K atoms at the same time. It is 0.03 eV higher in energy than **44A-I**, and its theoretical VDE is 1.50 eV, close to the experimental VDE (1.58 eV) of feature X″. Isomer **44A-IV** can be viewed as a double "V" like structure, and it is higher in energy than **44A-I** by 0.05 eV with a theoretical VDE of 1.46 eV. The other isomers like **44A-III**, **44A-V**, and **44A-VI** are all somewhat similar to **44A-II** and can also be derived from isomer **33A-I**. Their relative stabilities and calculated VDEs are summarized in Table 2. As we mentioned earlier, the three spectral features observed in the 532 nm spectrum of $(KI)_4^-$ should come from different isomers. By comparing the calculated VDEs and the experimental values, we suggest that the X feature is contributed by isomer **44A-I**; the X′ feature is mainly contributed by isomer **44A-V**, while the X″ feature is mainly contributed by isomers **44A-II** and **44A-VI**. Besides, isomer **44A-III** may contribute to the rising onset of feature X′ which extends from 0.6 to 1.2 eV. Note that we have also tried to verify the existence of multiple isomers for $(KI)_3^-$ and $(KI)_4^-$ using the isomer-depletion method. However, the results are not certain because the X′ and X″ features are also depleted significantly, probably due to the photodissociation or two-photon detachment of the higher-ADE isomers of $(KI)_3^-$ and $(KI)_4^-$ by the 1064 nm laser. The most stable isomer of neutral $(KI)_4$ (**44N-I**) is also a cubic structure, representing the smallest structural motif of face-centered cubic (FCC) KI crystal. This isomer is very similar to **44A-I** with slightly shorter K−I bond length (3.43 vs 3.47 Å). We noted here that our calculated K−I bond length (3.43 Å) in cubic $(KI)_4$ is close to the one (3.398 Å) calculated by EI-Hamdi et al. at the BP86/QZ4P level of theory.[32] The ladder-like structure (**44N-II**) is 0.68 eV higher in energy than the cubic structure. Isomer **44N-III** is 0.80 eV higher in energy than **44N-I**. Isomer **44N-IV** has a ring structure and is higher in energy than **44N-I** by 0.90 eV.

4.2. $K(KI)_n^{-/0}$ (n = 1−3). For $K(KI)^-$, we obtained two low-lying isomers, **21A-I** and **21A-II**, with **21A-II** being 0.17 eV higher in energy. Isomer **21A-I** is linear with two K atoms directly interacting with each other at a distance of 4.27 Å, and the K−I distance is 3.26 Å. As will be shown later, both the terminal K (−0.602 e) and I (−0.879 e) atoms of isomer **21A-I** are negatively charged, whereas the middle K (+0.481 e) atom is positively charged. Hence, the two K atoms prefer to interact with each other. Its theoretical VDE is 1.34 eV, close to the value of 1.41 eV measured from the X′ feature. Isomer **21A-II** is an isosceles triangle with K−I bond length of 3.42 Å and K−K distance of 4.02 Å. Its VDE is calculated to be 0.68 eV, in agreement with the experimental value of 0.78 eV measured

DOI: 10.1021/acs.jpca.5b09205
J. Phys. Chem. A 2015, 119, 11154−11161

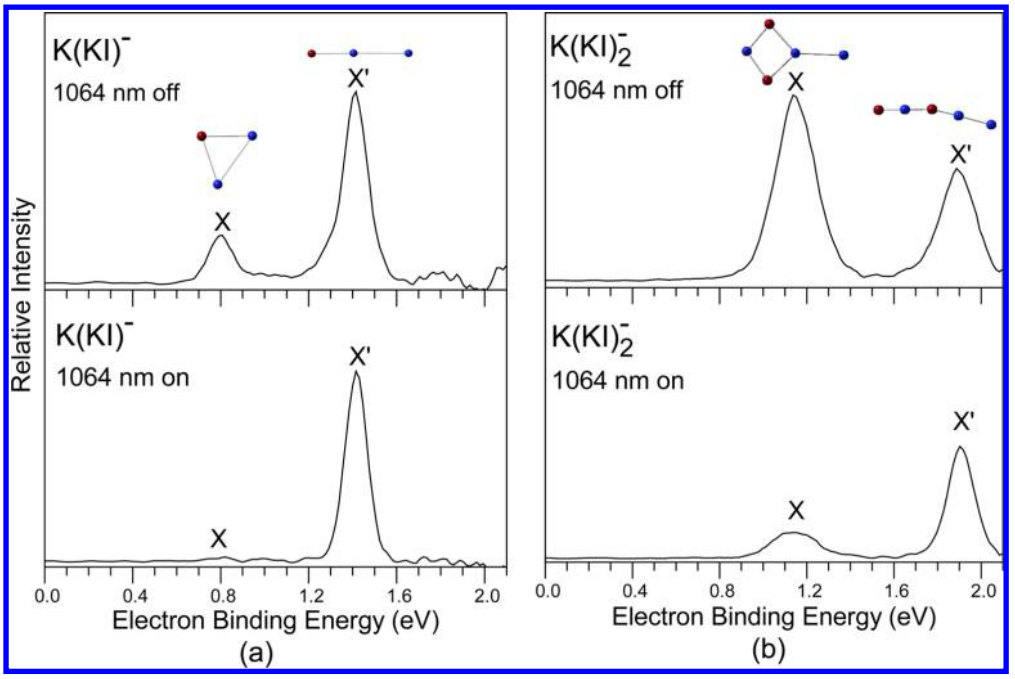

Figure 6. Isomer-depletion experiments on $K(KI)^-$ and $K(KI)_2^-$ clusters confirm that the X and X′ features are from different isomers. (a) Photoelectron spectra of $K(KI)^-$ at 532 nm with 1064 nm depletion laser off (top) and on (bottom). (b) Photoelectron spectra of $K(KI)_2^-$ at 532 nm with 1064 nm depletion laser off (top) and on (bottom). The isomers contributing to the respective spectral features are inserted. (The spectra are normalized based on the intensities of the X′ features. It is worth mentioning that the intensities of the X′ features also decreased when the 1064 nm laser was on, probably due to the photodissociation or two-photon detachment of the higher-ADE isomers by the 1064 nm laser.)

from the X feature. Hence, isomers **21A-I** and **21A-II** may coexist in the experiments. In order to confirm that the X and X′ features are indeed from different isomers, we conducted isomer-depletion experiments, in which the lower-ADE isomer (X feature) was depleted by a 1064 nm laser beam before the anions were photodetached by a 532 nm laser beam. It can be seen from Figure 6a that when the 1064 nm depletion laser is off, the photoelectron spectrum of $K(KI)^-$ is the same as the one shown in Figure 2. However, when the 1064 nm depletion laser is on, the relative intensities between the X and X′ features changes significantly with the X feature almost gone. This provides direct experimental evidence that the X and X′ features are contributed by isomers **21A-II** and **21A-I**, respectively. For neutral K(KI), we obtained two low-lying isomers **21N-I** and **21N-II**, with 0.24 eV energy difference. Isomer **21N-I** is an isosceles triangle with K−I bond length of 3.30 Å and K−K distance of 4.26 Å. This is quite different from **21A-I** due to the electrostatic repulsion between K and I atoms in its anionic state. Isomer **21N-II** is quasi-linear with the I atom interacting with the two K atoms both at a distance of 3.27 Å.

The ground state structure of $K(KI)_2^-$ (**32A-I**) is quasi-linear and can be deduced from **22A-I** by attaching the K atom to the K side of 22A-I through K−K interaction. The theoretical VDE of **32A-I** is 1.74 eV, close to the value of 1.89 eV measured for feature X′. Isomer **32A-II** has a kitelike configuration and can be viewed as attaching the K atom to **22A-II** via K−K interaction. It is 0.06 eV higher in energy than **32A-I**, and its VDE is calculated to be 1.00 eV, in good accordance with the experimental value of 1.13 eV from the X feature. Isomer **32A-III** has a "W-like" configuration and is 0.13 eV higher in energy than **32A-I**. Its theoretical VDE is 0.88 eV, much lower than the experimental results. The theoretical VDE of isomer **32A-IV** is 0.76 eV, also much lower than the experiments. Thus, we suggest that isomers **32A-I** and **32A-II** coexist in the experiments. We also conducted isomer-depletion experiments to verify the coexistence of isomers **32A-I** and **32A-II** and show the spectra in Figure 6b. It can be seen that the spectrum is similar to the one shown in Figure 2 when the 1064 nm depletion laser is off, but the relative intensities between the X and X′ features change significantly with the X feature being greatly suppressed when the 1064 nm depletion laser is on. This confirms that the X and X′ features in the experimental spectrum of $K(KI)_2^-$ are contributed by isomers **32A-II** and **32A-I**, respectively. The X feature did not totally disappear because the ion beam of isomer **32A-II** was not depleted completely by the 1064 nm laser. For the neutral $K(KI)_2$, three low-lying isomers are presented in Figure 5. The ground state structure **32N-I** can be evolved from **22N** with the K atom forming a triangle with one side of the rhombus $(KI)_2$. This is different from the quasi-linear structure of the most stable isomer of $K(KI)_2^-$ anion. The reason why the structures are different should be similar as in the $(KI)_2^{-/0}$ case. Isomer **32N-II** (+0.05 eV) is similar to **32A-III** and isomer **32N-III** is similar to **32A-II**, but isomer **32N-III** has much higher energy than **32N-I** by 0.28 eV.

The most stable structure of $K(KI)_3^-$ (**43A-I**) can be deduced from **33A-I** by attaching the K atom to **33A-I** through interacting with the two less coordinated (to I atom) K atoms at the same time. Its theoretical VDE is 1.63 eV, in good agreement with the experimental value of 1.71 eV. The corresponding neutral structure of **43A-I** is a quasi-planar structure (**43N-IV** in Figure 5), much different from the structure of **43A-I**. This agrees with the observation of the long rising onset in the 532 nm photoelectron spectrum of $K(KI)_3^-$. Isomer **43A-II** has a fishlike structure, and it is 0.08 eV higher in energy than **43A-I**. Its calculated VDE is 1.33 eV, consistent with the rising edge in the range of 1.2−1.6 eV in the

DOI: 10.1021/acs.jpca.5b09205
J. Phys. Chem. A 2015, 119, 11154−11161

experimental spectrum of the $K(KI)_3^-$. Thus, isomer **43A-II** may also exist in the experiment. The relative energies and theoretical VDEs of isomers **43A-III** to **43A-VII** are summarized in Table 2, and their VDEs are all significantly smaller than the experimental value. The most stable isomer of neutral $K(KI)_3$ (**43N-I**) is similar to **43A-III** but much different from **43A-I**. This is because the excess electron in the anion will make one K atom negatively charged, and thus it will prefer to interact with the positively charged K atoms, while in the neutral state all K atoms are positively charged and will prefer to interact with the negatively charged I atoms. Isomer **43N-II** is a ladder-like structure and can be derived from **33N-I**, and it is 0.20 eV higher in energy than **43N-I**.

4.3. Bonding Properties and Cluster Stabilities. To explore the bonding nature between K and I atoms and the excess electron binding properties in these clusters, the NBO charge distributions, molecular orbitals (MOs), and electron localization functions (ELFs)[33] analyses for the most probable structures were performed.

The NBO charge analyses (Figure S6) show that the excess electron e^- is mainly localized at the less coordinated (to I atoms) K atoms for $K(KI)_n^-$ and $(KI)_n^-$ (n = 1−3) clusters; while for $(KI)_4^-$, the excess electron has been evenly distributed at the four K atoms as they have identical coordination environments. The distributions of the excess electron in these clusters can be more clearly seen from the HOMOs of $K(KI)_n^-$ and the singly occupied molecular orbitals (SOMOs) of $(KI)_n^-$ as shown in Figure 7. It can be seen that these HOMOs/SOMOs are mainly composed of the s orbitals of the K atoms, implying that the excess electrons in these clusters are loosely bound. These phenomena are consistent with the low EBEs of these clusters measured from the experiments. More interesting is that for $K(KI)_n^-$ clusters, there is a single K atom in each size cluster possessing most of the excess electron; hence, the excess electron in the $K(KI)_n^-$ clusters occupies the s orbital and form an electron pair with the existing s electron of the K atom. The analyses confirm the suggestion made by Smalley and co-workers that in K-rich clusters the excess electrons are loosely bound and electron spin pairs may form.[16] Besides, the ELFs analyses (Figure S6) clearly show strong ionic bonding interactions between K and I atoms. The strong ionic bonding makes K or I atom interact with as many as their counterions simultaneously, and thus cubic structure will be the most preferable configuration for $(KI)_4^{-/0}$ to fulfill this demand.

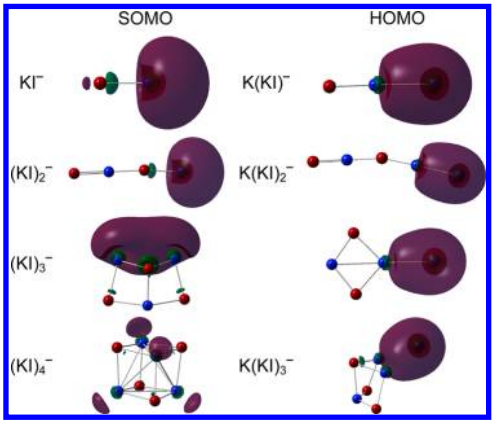

Figure 7. Singly occupied molecular orbitals (SOMOs) of $(KI)_n^-$ and the highest occupied molecular orbitals (HOMOs) of $K(KI)_n^-$. The blue and purple balls represent K and I atoms, respectively.

In these clusters, $(KI)_n$ neutrals may be more relevant to the KI crystal structure. Therefore, we evaluated their MOs (Figure S7) and found that the HOMOs are mainly composed of the I p orbitals, while the LUMOs are mainly contributed by the K s obtials where the s electrons are grabbed by the I atoms. The HOMO−LUMO gaps of the $(KI)_n$ neutral clusters are all larger than 3.2 eV, which may reflect their high-stability nature toward reactions. Besides, the calculated large HOMO−LUMO gaps also confirm our above analyses that the multiple features observed in the spectra of $(KI)_3^-$ and $(KI)_4^-$ come from different isomers in the cluster beams. Specifically, for KI, the calculated HOMO−LUMO gap is 3.25 eV, in agreement with the experimental value of 3.45 eV measured from the 266 nm spectrum of KI^- (Figure S1). For $(KI)_4$, it has a very large HOMO−LUMO gap of 5.15 eV. Further calculation on its dissociation energy with respect to dissociate into 4(KI) and $(KI)_3$ + KI provides values of 4.90 and 2.00 eV respectively at the B3LYP level of theory. Both the large HOMO−LUMO gap and the relatively large dissociation energy indicate the high stability of cuboid $(KI)_4$ cluster.

5. CONCLUSIONS

Potassium-iodide clusters $(KI)_n^-$ (n = 1−4) and $K(KI)_n^-$ (n = 1−3) as well as their neutrals were investigated by negative ion photoelectron spectroscopy and ab initio calculations. The VDEs and ADEs of these clusters were determined from their photoelectron spectra. By comparing the theoretical VDEs with the experimental values, the most probable structures of these clusters were identified. Direct experimental evidence was obtained for the existence of multiple isomers in the cluster beam. Due to the effect of different charges, the most stable structures of the $K(KI)^-$, $(KI)_2^-$, and $K(KI)_2^-$ anions are chain structures while those of their neutral counterparts are planar. Three-dimensional structures start to appear at n = 3 for $(KI)_n^{-/0}$ and $K(KI)_n^{-/0}$. In the $K(KI)_n^-$ (n = 1−3) cluster anion, the excess electron is localized on the extra K atom and forms an electron pair with the existing s electron of K atom; the resulting negatively charged K prefers to interact with the other K atoms which are positively charged instead of with the negatively charged I atoms. In neutral $K(KI)_n$, the extra K prefers to interact with the negatively charged I atoms. The structural difference between the anionic and neutral clusters becomes less obvious with increasing cluster size. In particular, the anionic and neutral $(KI)_4$ clusters are both cubic and may be considered as the smallest structural motif of KI crystal.

■ ASSOCIATED CONTENT

Supporting Information

The Supporting Information is available free of charge on the ACS Publications website at DOI: 10.1021/acs.jpca.5b09205.

The 266 nm photoelectron spectra of $(KI)_n^-$ (n = 1−4) and $K(KI)_n^-$ (n = 1−3) clusters, conditions-varied photoelectron spectra of $(KI)_3^-$ and $(KI)_4^-$, more isomers of $(KI)_n^-$ (n = 1−4) and $K(KI)_n^-$ (n = 1−3) and their neutrals, as well as the NBO charge distributions, ELFs, and MOs analyses (PDF)

■ AUTHOR INFORMATION

Corresponding Author

*Phone: +86-10-62635054. E-mail: zhengwj@iccas.ac.cn.

DOI: 10.1021/acs.jpca.5b09205
J. Phys. Chem. A 2015, 119, 11154−11161

Notes

The authors declare no competing financial interest.

■ ACKNOWLEDGMENTS

This work was supported by the National Natural Science Foundation of China (Grant No. 21403249 to G.F. and 21273246 to W.J.Z.). The theoretical calculations were conducted on the ScGrid and DeepComp 7000 of the Supercomputing Center, Computer Network Information Center of Chinese Academy of Sciences.

■ REFERENCES

(1) Martin, T. P. Alkali Halide Clusters and Microcrystals. *Phys. Rep.* **1983**, *95*, 167−199.
(2) Barlak, T. M.; Wyatt, J. R.; Colton, R. J.; DeCorpo, J. J.; Campana, J. E. Secondary Ion Mass Spectrometry of Metal Halides. 2. Evidence for Structure in Alkali Iodide Clusters. *J. Am. Chem. Soc.* **1982**, *104*, 1212−1215.
(3) Beck, R. D.; John, P. S.; Homer, M. L.; Whetten, R. L. Impact-Induced Cleaving and Melting of Alkali-Halide Nanocrystals. *Science* **1991**, *253*, 879−883.
(4) Phillips, N. G.; Conover, C. W. S.; Bloomfield, L. A. Calculations of the Binding Energies and Structures of Sodium Chloride Clusters and Cluster Ions. *J. Chem. Phys.* **1991**, *94*, 4980−4987.
(5) Ayuela, A.; Lopez, J. M.; Alonso, J. A.; Luana, V. Theoretical Study of $(NaCl)_n$ Clusters. *Phys. B* **1995**, *212*, 329−342.
(6) Aguado, A.; Ayuela, A.; Lopez, J. M.; Alonso, J. A. Theoretical Study of Small $(NaI)_n$ Clusters. *J. Phys. Chem. B* **1997**, *101*, 5944−5950.
(7) Malliavin, M. J.; Coudray, C. Ab Initio Calculations on $(MgO)_n$, $(CaO)_n$, and $(NaCl)_n$ Clusters (n = 1−6). *J. Chem. Phys.* **1997**, *106*, 2323−2330.
(8) Aguado, A. An ab Initio Study of the Structures and Relative Stabilities of Doubly Charged $[(NaCl)_m(Na)_2]^{2+}$ Cluster Ions. *J. Phys. Chem. B* **2001**, *105*, 2761−2765.
(9) Veličković, S. R.; Veljković, F. M.; Perić-Grujić, A. A.; Radak, B. B.; Veljković, M. V. Ionization Energies of K_2X (X = F, Cl, Br, I) Clusters. *Rapid Commun. Mass Spectrom.* **2011**, *25*, 2327−2332.
(10) Veljković, F. M.; Djustebek, J. B.; Veljković, M. V.; Perić-Grujić, A. A.; Veličković, S. R. Study of Small Chlorine-Doped Potassium Clusters by Thermal Ionization Mass Spectrometry. *J. Mass Spectrom.* **2012**, *47*, 1495−1499.
(11) Ohshimo, K.; Takahashi, T.; Moriyama, R.; Misaizu, F. Compact Non-Rock-Salt Structures in Sodium Fluoride Cluster Ions at Specific Sizes Revealed by Ion Mobility Mass Spectrometry. *J. Phys. Chem. A* **2014**, *118*, 9970−9975.
(12) Daxner, M.; Denifl, S.; Scheier, P.; Ellis, A. M. Electron-Driven Self-Assembly of Salt Nanocrystals in Liquid Helium. *Angew. Chem., Int. Ed.* **2014**, *53*, 13528−13531.
(13) Yang, Y. A.; Conover, C. W. S.; Bloomfield, L. A. Production and Photodetachment of Stoichiometric Sodium Chloride Cluster Anions. *Chem. Phys. Lett.* **1989**, *158*, 279−282.
(14) Wang, X.-B.; Ding, C.-F.; Wang, L.-S.; Boldyrev, A. I.; Simons, J. First Experimental Photoelectron Spectra of Superhalogens and Their Theoretical Interpretations. *J. Chem. Phys.* **1999**, *110*, 4763−4771.
(15) Alexandrova, A. N.; Boldyrev, A. I.; Fu, Y.-J.; Yang, X.; Wang, X.-B.; Wang, L.-S. Structure of the $Na_xCl_{x+1}^-$ (x = 1−4) Clusters via ab Initio Genetic Algorithm and Photoelectron Spectroscopy. *J. Chem. Phys.* **2004**, *121*, 5709−5719.
(16) Yang, Y. A.; Bloomfield, L. A.; Jin, C.; Wang, L. S.; Smalley, R. E. Ultraviolet Photoelectron Spectroscopy and Photofragmentation Studies of Excess Electrons in Potassium Iodide Cluster Anions. *J. Chem. Phys.* **1992**, *96*, 2453−2459.
(17) Xia, P.; Bloomfield, L. A. Evidence for a Phase Separation in Metal-Rich Alkali-Halide Cluster Anions. *Phys. Rev. Lett.* **1994**, *72*, 2577−2580.
(18) Xu, H.-G.; Zhang, Z.-G.; Feng, Y.; Yuan, J. Y.; Zhao, Y. C.; Zheng, W. J. Vanadium-Doped Small Silicon Clusters: Photoelectron Spectroscopy and Density-Functional Calculations. *Chem. Phys. Lett.* **2010**, *487*, 204−208.
(19) Akin, F. A.; Jarrold, C. C. Separating Contributions from Multiple Structural Isomers in Anion Photoelectron Spectra: $Al_3O_3^-$ Beam Hole Burning. *J. Chem. Phys.* **2003**, *118*, 1773−1778.
(20) Frisch, M. J.; Trucks, G. W.; Schlegel, H. B. *Gaussian 09*; Gaussian Inc.: Wallingford, CT, 2009.
(21) Lee, C.; Yang, W.; Parr, R. G. Development of the Colle-Salvetti Correlation-Energy Formula into a Functional of the Electron Density. *Phys. Rev. B: Condens. Matter Mater. Phys.* **1988**, *37*, 785−789.
(22) Becke, A. D. Density-functional Thermochemistry. III. The Role of Exact Exchange. *J. Chem. Phys.* **1993**, *98*, 5648−5652.
(23) Krishnan, R.; Binkley, J. S.; Seeger, R.; Pople, J. A. Self−Consistent Molecular Orbital Methods. XX. A Basis Set for Correlated Wave Functions. *J. Chem. Phys.* **1980**, *72*, 650−654.
(24) Hou, G.-L.; Wu, M. M.; Wen, H.; Sun, Q.; Wang, X.-B.; Zheng, W.-J. Photoelectron Spectroscopy and Theoretical Study of $M(IO_3)_2^-$ (M = H, Li, Na, K): Structural Evolution, Optical Isomers, and Hyperhalogen Behavior. *J. Chem. Phys.* **2013**, *139*, 044312−7.
(25) ESML Basis Set Exchange. https://bse.pnl.gov/bse/portal.
(26) Rice, S. A.; Klemperer, W. Spectra of the Alkali Halides. II. The Infrared Spectra of the Sodium and Potassium Halides, RbCl, and CsCl. *J. Chem. Phys.* **1957**, *27*, 573−579.
(27) Miller, T. M.; Leopold, D. G.; Murray, K. K.; Lineberger, W. C. Electron Affinities of the Alkali Halides and the Structure of Their Negative Ions. *J. Chem. Phys.* **1986**, *85*, 2368−2375.
(28) Honig, A.; Mandel, M.; Stitch, M.; Townes, C. Microwave Spectra of the Alkali Halides. *Phys. Rev.* **1954**, *96*, 629−642.
(29) Sunil, K. K.; Jordan, K. D. Negative Ion Formation in Alkali Halide Clusters. *J. Phys. Chem.* **1987**, *91*, 1710−1711.
(30) Anusiewicz, I.; Skurski, P.; Simons, J. First Evidence of Rhombic $(NaCl)_2^-$. Ab Initio Reexamination of the Sodium Chloride Dimer Anion. *J. Phys. Chem. A* **2002**, *106*, 10636−10644.
(31) Gutsev, G. L.; Jena, P.; Bartlett, R. J. Search for "Quadrupole-Bound" Anions. I. *J. Chem. Phys.* **1999**, *111*, 504−511.
(32) El-Hamdi, M.; Solà, M.; Frenking, G.; Poater, J. Comparison between Alkalimetal and Group 11 Transition Metal Halide and Hydride Tetramers: Molecular Structure and Bonding. *J. Phys. Chem. A* **2013**, *117*, 8026−8034.
(33) Lu, T.; Chen, F. Multiwfn: A Multifunctional Wavefunction Analyzer. *J. Comput. Chem.* **2012**, *33*, 580−592.

DOI: 10.1021/acs.jpca.5b09205
J. Phys. Chem. A 2015, 119, 11154−11161